Pair Correlations in Liquid and Solid Aluminum†

R. R. FESSLER,* ROY KAPLOW, AND B. L. AVERBACH
Department of Metallurgy, Massachusetts Institute of Technology, Cambridge, Massachusetts
(Received 2 May 1966)

Radial density functions were determined by x-ray diffraction for solid aluminum at 25, 325, and 655°C and for liquid aluminum at 665 and 750°C. Computer techniques were used to minimize the effects of experimental errors, of uncertainties in the scattering factors, and of termination errors. It was assumed that the thermal atomic displacements in solid aluminum follow a Gaussian distribution, and the resultant Debye temperatures were 383, 362, and 322°K for specimens at 25, 325, and 655°C. The first ten coupling factors, averaged for the three temperatures, were 0.70, 0.73, 0.92, 0.90, 0.82, 0.83, 1.00, 0.96, 0.93, 0.93. The radial density functions of liquid aluminum at 665 and 750°C were quite similar. Liquid aluminum has the same basic structure as liquid lead, but a different structure from that of liquid mercury. Comparisons with the random packing model showed that this model does not reproduce the details of the measured radial density function. A quasicrystalline model, in which the radial density function of the solid is broadened and damped by the introduction of a cell size and liquid diffusive motions, agreed quite well with the experimental density function. A tunnel model, in which atoms move freely in tunnels arranged in a two-dimensional close-packed network, also fitted quite well, but a large number of free parameters is required.

I. INTRODUCTION

THE availability of accurate radial density functions of liquids has been helpful in efforts to derive analytical descriptions of the structure of liquids. The method used here depends on obtaining rather extensive x-ray diffraction data and then using a computer method to reduce the uncertainties in normalization and to minimize the termination errors. The resultant radial distribution functions exhibit details which are quite reliable and are characteristic of the liquid. We have also treated diffraction data from the solid in the same fashion, and the subsequent comparison between the liquid and solid distribution functions provides considerable insight into the structure of the liquid.

Although radial density functions for liquid aluminum have been measured before,[1–5] there are marked discrepancies in the results. For comparison, we have plotted in Fig. 1 various determinations of the reduced radial density function, which is defined as

$$H(r)=4\pi r^2[\rho(r)-\rho_0], \qquad (1)$$

where r is the radial correlation distance, $\rho(r)$ is the number of atoms per unit volume at distance r from a given atom, and ρ_0 is the average density of atoms in the system. Of the results shown in this figure, Gamertsfelder,[1] Dutchak,[2] and Black and Cundall[3] used x-ray diffraction, whereas Bublik and Buntar[4] used electron diffraction. Although Black and Cundall claim agreement with Gamertsfelder, there appear to be serious discrepancies between those two sets of data. Ruppersberg and Seemann[5] present a table of maxima and minima positions for the reduced x-ray intensity function which are close to those obtained by Garmetsfelder. Their results are not given in sufficient detail, however, to allow a quantitative comparison. The discrepancies between the various measurements are probably due in part to differences in experimental techniques and to the resultant experimental errors, but significant errors may have also been introduced by the analysis.

Two factors are important in lending some confidence in the present results: (1) the development of a computer-aided technique[6] for eliminating termination and systematic experimental errors, and (2) the use of improved apparatus for the x-ray intensity measurements.[7]

II. EXPERIMENTAL PROCEDURE

Diffraction patterns were obtained from sintered aluminum powder of 99.99+% purity at 25, 325, and 655°C and from liquid aluminum of the same purity at 665 and 750°C. The liquid aluminum was held in an alumina crucible which provided a $1\frac{3}{4}$ by $1\frac{1}{4}$ in. surface. In order to minimize the effect of the curved meniscus of the liquid aluminum on the x-ray geometry, the linear dimensions of the beam on the specimen surface were always kept to less than half the dimensions of the surface. The specimen surface remained horizontal in an enclosed high-temperature stage of a diffractometer which was driven at a constant $d(\sin\theta)/dt$. Equal angles of incidence and reflection were maintained between the x-ray beams and the specimen surface.

† Sponsored by the U. S. Office of Naval Research, Contract Nonr-1841(48).
* Present address: Battelle Memorial Institute, Columbus, Ohio.
[1] C. Gamertsfelder, J. Chem. Phys. **9**, 450 (1941).
[2] Ya. I. Dutchak, Kristallografiya **6**, 124 (1961) [English transl.: Soviet Phys.—Crystallography **6**, 100 (1961)].
[3] P. J. Black and J. A. Cundall, Acta Cryst. **19**, 807 (1965).
[4] A. I. Bublik and A. G. Buntar, Phys. Metals Metallog. **5**, 41 (1957).
[5] H. Ruppersberg and H. J. Seemann, Z. Naturforsch. **20a**, 104 (1965).
[6] R. Kaplow, S. L. Strong, and B. L. Averbach, Phys. Rev. **138**, A1336 (1965).
[7] R. Kaplow and B. L. Averbach, Rev. Sci. Instr. **34**, 579 (1963).

The positions of the low-angle reflections are very sensitive to slight displacements of the specimen surface from the spectrometer axis, and the solid aluminum specimen was positioned by requiring that the (111) reflection occur at the angle calculated from the known lattice parameter. Positioning of the liquid specimen was accomplished in a similar fashion by adjusting the angle of the (200) reflection from small particles of MgO which were floated on the surface of the specimen. The MgO powder was removed after the correct alignment conditions had been established. The furnace windings were protected from oxidation by maintaining an atmosphere of purified hydrogen, which also served to minimize oxidation of the aluminum.

Mo $K\alpha$ radiation was monochromated by using the (111) reflection from a bent silicon single crystal located in the incident beam. The diffracted radiation passed through 3° lateral Soller slits in order to minimize the effects of vertical divergence. The diffracted intensity was detected by a scintillation counter in conjunction with a pulse-height analyzer and was recorded continuously with a counting rate meter and strip-chart recorder. Four successive intensity profiles were measured at each temperature alternately in directions of increasing and decreasing $\sin\theta$ in order to improve the accuracy of the data.

III. ANALYSIS OF THE DATA

The relationship between the radial density function and the diffracted intensity may be written[8]

$$G(r)=H(r)/r=(2/\pi)\int_0^\infty F(k)\sin krdk, \qquad (2)$$

where the intensity function, $F(k)=k(I-f^2)/f^2$. Here I is the coherently diffracted intensity per atom in electron units, f^2 is the product of the atomic scattering factor and its conjugate, $k=(4\pi\sin\theta)/\lambda$, θ is the diffraction angle, and λ is the wavelength of the radiation. The function $G(r)$ is called the distribution function.

The measured intensity is related to the absolute intensity by

$$I=(AI_m/P)-I_c, \qquad (3)$$

where I_m is the total diffracted intensity in arbitrary units, A is a normalizing factor which converts the intensity to electron units, P is the polarization factor, and I_c is the Compton modified intensity in electron units.

If the angles of incidence and reflection between the x-ray beams and the sample are equal, and the receiver geometry is such that the detector senses diffracted radiation from all irradiated portions of the sample, the effect of absorption on the integrated intensities of the peaks is independent of k and can be incorporated into the normalization constant. However, in the case of materials with low absorption, the shape of the diffraction pattern is distorted in a manner described by Alexander[9] because of the diffraction from portions of the specimen appreciably below the surface. The peak shapes were corrected numerically with the aid of a computer program. Although the corrections were appreciable for the solid aluminum specimens, they were negligible for the diffuse scattering from the liquid.

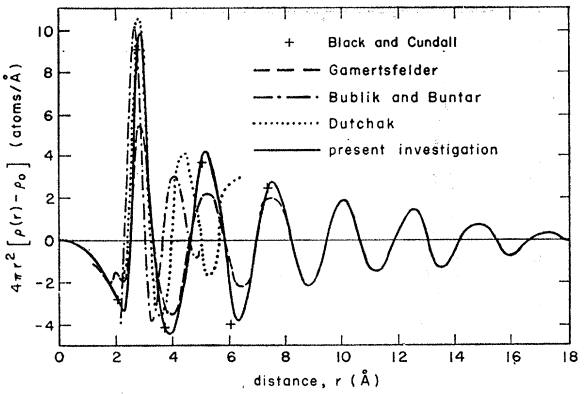

FIG. 1. Radial density functions, $4\pi r^2(\rho(r)-\rho_0)$, reported for liquid aluminum. Points shown for B and C are uncorrected maxima and minima obtained from their CuK_α data.

The normalization constant may be written

$$A=P(I_c+f^2)/I_m+P(f^2F(k)/k)/I_m. \qquad (4)$$

The quantity $F(k)$ oscillates about zero, and the expression $P(I_c+f^2)/I_m$ should oscillate about the normalization constant, A. Using the usual dispersion corrections,[8] Hartree-Fock-Slater atomic scattering factors,[10] Compton modified scattering intensities with the Breit-Dirac correction,[11] and the experimental diffracted intensity from liquid aluminum, it was found that the normalization function, Eq. (4), did not oscillate about a constant value but increased monotonically with increasing scattering angle. The deviation from a constant value was nearly the same for both sets of liquid data, and this suggested that the theoretical values of (I_c+f^2) are probably not correct. Therefore, the measured intensity was used to adjust the values of (I_c+f^2) so that a constant normalization factor was obtained. These adjusted values also compensated for any systematic errors which might have existed in the high-angle intensity data. If the slowly varying error is attributed entirely to an erroneous (I_c+f^2) shape, then the required corrections amount to about 5% of the theoretical values. A portion of this error, however, might be due to an oxide film on the surface. The correct normalization constant was determined by a method which takes advantage of the

[8] R. W. James, *The Optical Principles of the Diffraction of X-Rays* (G. Bell and Sons, London, 1958).

[9] L. Alexander, J. Appl. Phys. **21**, 126 (1950).

[10] H. P. Hanson, F. Herman, J. D. Lea, and S. Skillman, Acta Cryst. **17**, 1040 (1964).

[11] A. J. Freeman, Phys. Rev. **113**, 176 (1959).

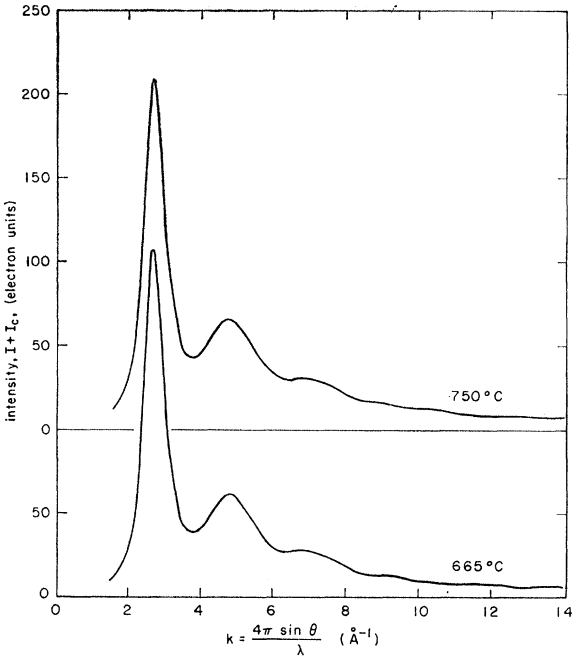

FIG. 2. Corrected total intensities, $I+I_c$, diffracted from liquid aluminum.

fact that an error in A will cause sharp oscillations very close to the origin in the calculated radial distribution function.[6] The normalized intensity diffracted from liquid aluminum is shown in Fig. 2.

The function $F(k)$ was transformed with a computer program, and it was observed that oscillations in the initial portion of $G(r)$ were present, indicating that errors existed in $F(k)$. A method for eliminating errors in I_m and f has been developed for the case where Compton modified scattering is negligible.[6] The Compton modified scattering was not eliminated experimentally in the present investigation, and the correction method was thus used only to eliminate errors in the low and intermediate regions of k where I_c is much smaller than f^2. Small errors at large values of k probably produce effects on $G(r)$ which are indistinguishable from termination error, and these errors were treated simultaneously.

Termination errors introduce extraneous oscillations in $G(r)$, primarily in the vicinity of the first correlation peak. This type of error arises because there is a practical experimental limit to the upper value of k, which we define as k_m. Our method[6] eliminates termination errors in radial distribution functions of liquids by generating an intensity function beyond k_m which is consistent with the measured intensity, and which eliminates the extraneous oscillations in $G(r)$. The resultant corrected intensity functions for liquid aluminum are shown in Fig. 3. The correction procedure described above requires that $G(r)$ approach zero at a value of r which is sufficiently small that its transform can be calculated without undue difficulty. While this is true for the liquid, in the case of the solid $G(r)$ is still appreciable at large values of r. After the experimental errors and errors in the theoretical scattering factors had been treated, extraneous oscillations in $G(r)$ were found in the vicinity of the first peak. These oscillations, which were more pronounced at lower temperatures, were clearly indicative of termination error, but could not be treated with the same certainty as in the case of the liquid. The corrected intensity functions for solid aluminum at 25 and 655°C are shown in Fig. 4.

Within the accuracy of the experimental measurements, the diffraction peaks, corrected for the absorption effect, exhibited a Gaussian shape with a constant half-width in k. Under these conditions, the effect of instrumental broadening is to exponentially damp the calculated distribution function by the factor, $\exp(-a^2r^2)$, where $a^2_2=\Delta^2(16\ln 2)$, and Δ is the full peak width at half-maximum.[12] The experimental distribution functions were corrected for this effect by using a value $a^2_2=1.765\times10^{-4}$ Å^{-2}, corresponding to the experimental peak width, $\sin\theta=0.0025$.

The final effect to be considered is that the radiation was not strictly monochromatic, since both the $K\alpha_1$ and the $K\alpha_2$ components were present. The measured $F(k)$ is thus the sum of two functions corresponding

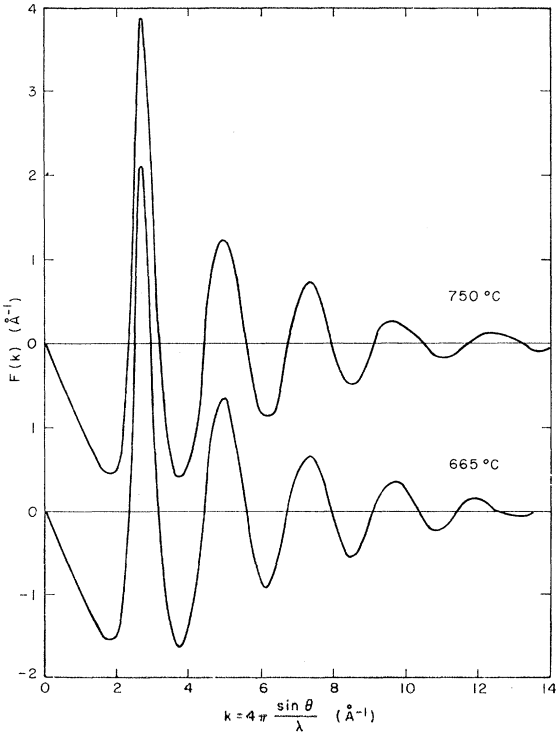

FIG. 3. Reduced intensity functions, $F(k)=k\{I/f^2-1\}$, for liquid aluminum.

[12] R. G. Lagneborg and R. Kaplow, Acta Met. (to be published).

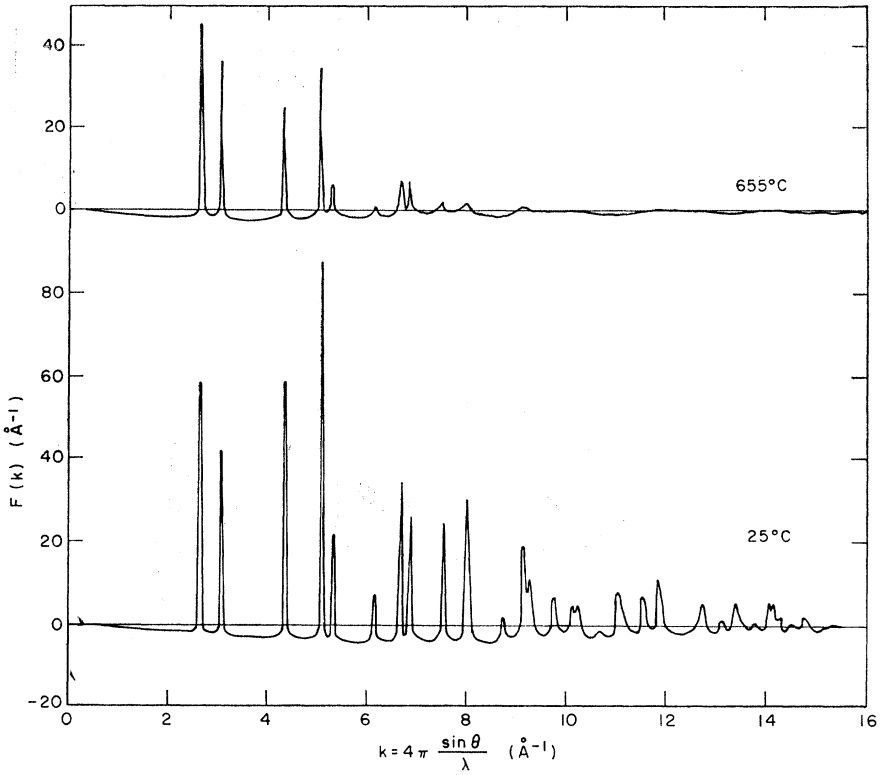

FIG. 4. Reduced intensity functions, $F(k)=k\{I/f^2-1\}$, for solid aluminum.

to two slightly different wavelengths. The calculated distribution function is the appropriately weighted sum of two distribution functions corresponding to the same structure but having slightly different lattice parameters. This effect was taken into account in the construction of the theoretical distribution functions with which the experimental functions were compared, rather than by using a complicated unfolding procedure on $F(k)$ or $G(r)$.

IV. DISCUSSION OF RESULTS

A. Solid Aluminum

The radial distribution function of a solid can be used to yield a considerable amount of information about the structure.[13] We assume that the radial density function may be written

$$4\pi r^2\rho(r)=\sum_{i=1}^{\infty} c_i/(2\pi\sigma^2\gamma_i)^{1/2}\exp[-(r-r_i)^2/2\sigma^2\gamma_i], \quad (5)$$

where c_i is the number of equilibrium atom positions located at a distance r_i from an average origin atom, σ^2 is the mean-square amplitude of relative vibration between a pair of distant atoms, and γ_i is a coupling factor which allows for a variation of the amplitude of relative vibration with the distance of separation.

[13] R. Kaplow, S. L. Strong, and B. L. Averbach, J. Phys. Chem. Solids 25, 1195 (1964).

In principle, the measured distribution function can be used to determine the crystal structure, because each structure possesses a unique set of c_i and r_i values. In the case of aluminum, which is known to have a fcc structure, selecting the correct c_i and r_i values was trivial. The excellent agreement between the theoretical distribution functions and the measured functions, as shown in Fig. 5, indicates that this approach provides an adequate representation of the solid structure. The calculated distribution functions are the weighted averages of two functions corresponding to the $K\alpha_1$ and $K\alpha_2$ components of the x rays. The positions of the oscillations in the calculated distribution functions are determined by the lattice parameter. The resultant values of the lattice parameter are 4.058, 4.091, and 4.123 Å for 25, 325, and 655°C, respectively. The sensitivity of the method is estimated to be about 0.005 Å. These values compare well with the values of 4.0490, 4.0806, and 4.123 Å calculated from the accepted value of 4.0490 Å at 20°C and an expansion coefficient of 27×10^{-6} per °C.

The Debye temperature may be computed from the measured value of σ, using the relationship

$$\Theta_0=(h/\sigma\pi)(3T/2mk)^{1/2}, \quad (6)$$

where Θ_0 is the Debye temperature, h is Planck's constant, T is the absolute temperature, m is the mass of the atom, and k is Boltzmann's constant. The

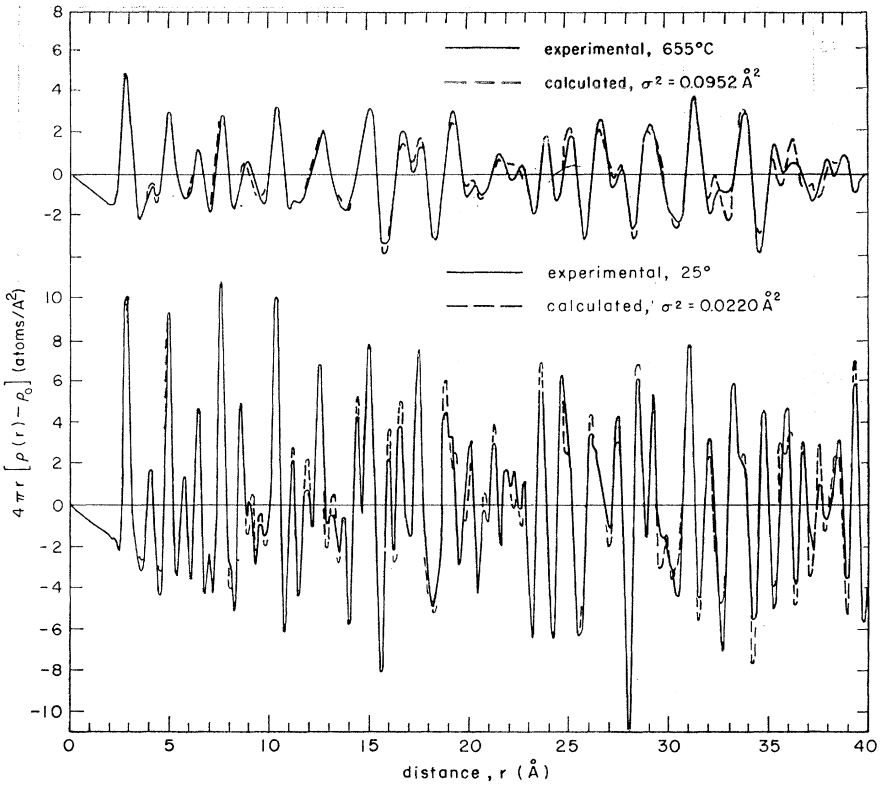

FIG. 5. Distribution functions, $4\pi r[\rho(r)-\rho_0]$, for solid aluminum.

value of σ^2 was determined by matching the heights of the oscillations in the calculated distribution function to the measured distribution function over the range of r from 20 to 39 Å, where the coupling factors γ_i are unity. The Debye temperatures of aluminum, calculated from Eq. (6), are shown in Fig. 6. It is evident that they compare well with previous calculations based on the effect of temperature on the integrated intensities of x-ray reflections[14,15] and on the effect of temperature on the elastic constants.[16]

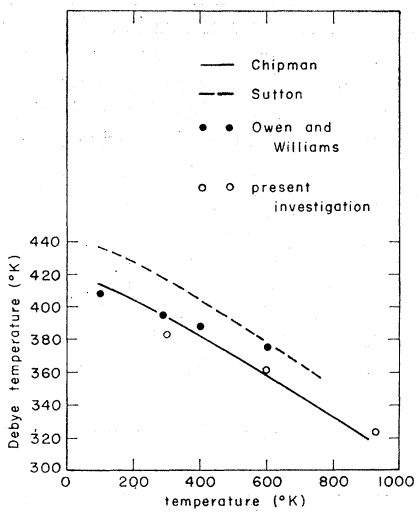

FIG. 6. Temperature variation of Debye temperature in solid aluminum.

The coupling factors, which were determined by matching the peak heights in the low-r portion of $G(r)$, exhibit considerable scatter when the results for the three temperatures are compared. The averages of the coupling factors for the three experiments thus may be more significant than the individual values. Figure 7 compares the averages with the predictions of Walker and Keating[17] which assume a linear chain dispersion relation. The two sets of values probably agree within the accuracy of the experiment. On the other hand, a trend in γ_1, which experimentally varies from 0.85 at 25°C to 0.55 at 655°C may be significant, particularly since the latter value is in excellent agreement with previous measurements of other fcc elements (lead and cobalt) at elevated temperatures.

Ruppersberg and Seemann[5] have also measured a radial distribution function for solid aluminum near the melting point. Their experimental result appears to be in essential agreement with ours. However, they do not provide values of coupling factors, and their stated disagreement, by a factor of 3, with Debye theory appears to arise from a confusion between the

[14] D. R. Chipman, J. Appl. Phys. **31**, 2012 (1960).
[15] E. A. Owens and R. W. Williams, Proc. Roy. Soc. (London) **A188**, 509 (1947).
[16] P. M. Sutton, Phys. Rev. **91**, 1816 (1953).
[17] C. B. Walker and D. T. Keating, Acta Cryst. **14**, 1170 (1960).

total mean-square amplitude of vibration and the component in a radial direction.

B. Liquid Aluminum

The radial density functions of liquid aluminum at 655 and 750°C are compared in Fig. 8. The positions of the oscillations are the same at both temperatures, but the amplitudes are slightly smaller at the higher temperature. A temperature difference of almost 100°C appears to have very little effect on the structure of of liquid aluminum.

The radial density function of liquid aluminum is compared in Fig. 9 with the previously measured density functions of lead, which also has a fcc solid structure, and mercury, which has a rhombohedral solid structure. In order to eliminate the irrelevant effect of atom size, the density functions are plotted as a function of nearest-neighbor distance r_1. This requires that the ordinate values be multiplied by r_1 in order to conserve the number of atoms. The coincidence of the positions of the oscillations for lead and aluminum indicates that the basic structures of these two liquids are similar. The difference in the amplitudes of the oscillations indicate a difference in the vibrational or diffusional characteristics, and these are probably influenced by the differences in the absolute temperatures and in the atomic masses. On the other hand, the comparison between mercury and aluminum shows that they have quite different liquid structures. These observations suggest that there is a correlation between the solid and liquid structures of metals.

Most theoretical calculations of the properties of liquids assume various arrangements of atoms. At present, however, there is no general agreement on the basic structure of liquids. In an attempt to assess the validity of several proposed theories, the present experimental results are compared with those models which are sufficiently developed to predict radial density functions. These models are the random packing model, the quasicrystalline model and the tunnel model.

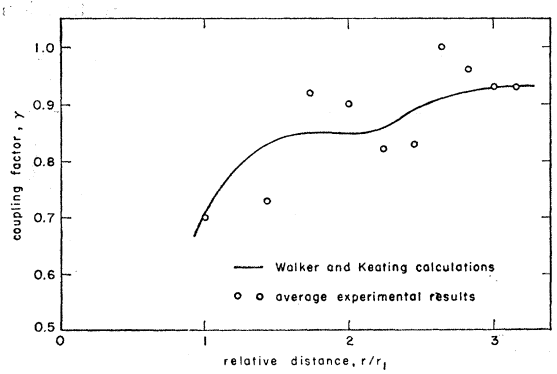

FIG. 7. Vibrational coupling factors in solid aluminum.

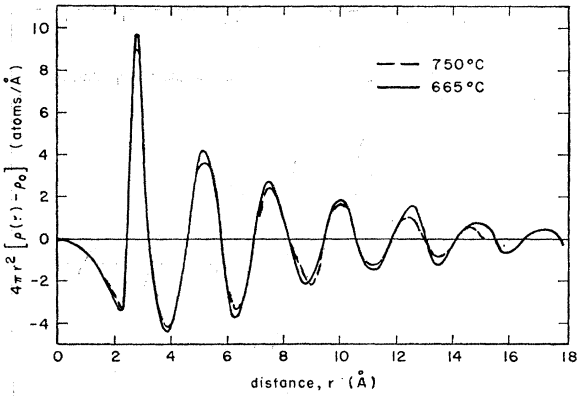

FIG. 8. Radial density functions, $4\pi r^2(\rho(r)-\rho_0)$, for liquid aluminum.

On the basis of a comparison of the structure of liquid argon with the distribution function of a dense disordered arrangement of identical spheres, Bernal[18] has proposed that the atoms in a simple liquid are arranged as randomly as possible consistent with the density of the liquid. Unfortunately, the differences between the experimental and randomly packed structures were de-emphasized by plotting $\rho(r)$ instead of $H(r)$. In Fig. 10(a), the measured density function of liquid aluminum is compared with the density

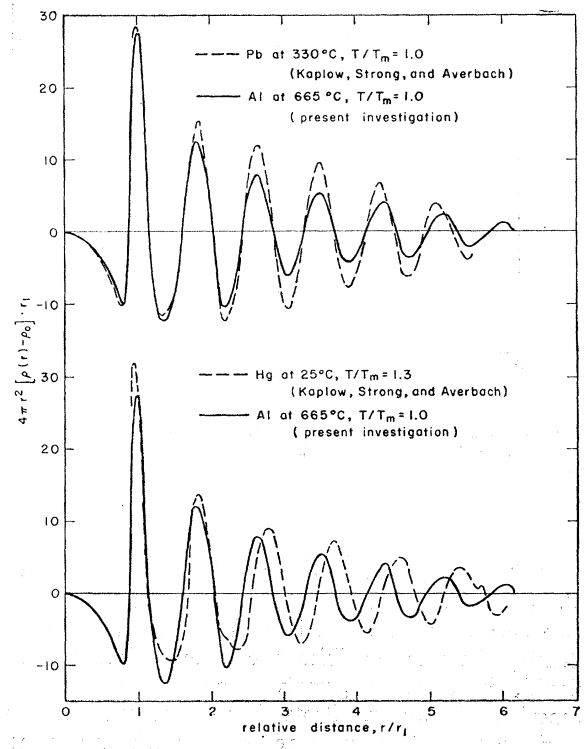

FIG. 9. Comparison of radial density functions of aluminum, lead, and mercury.

[18] J. D. Bernal, *Liquids: Structure, Properties, Solid Interactions* (Elsevier Publishing Company, Inc., New York, 1965), p. 25.

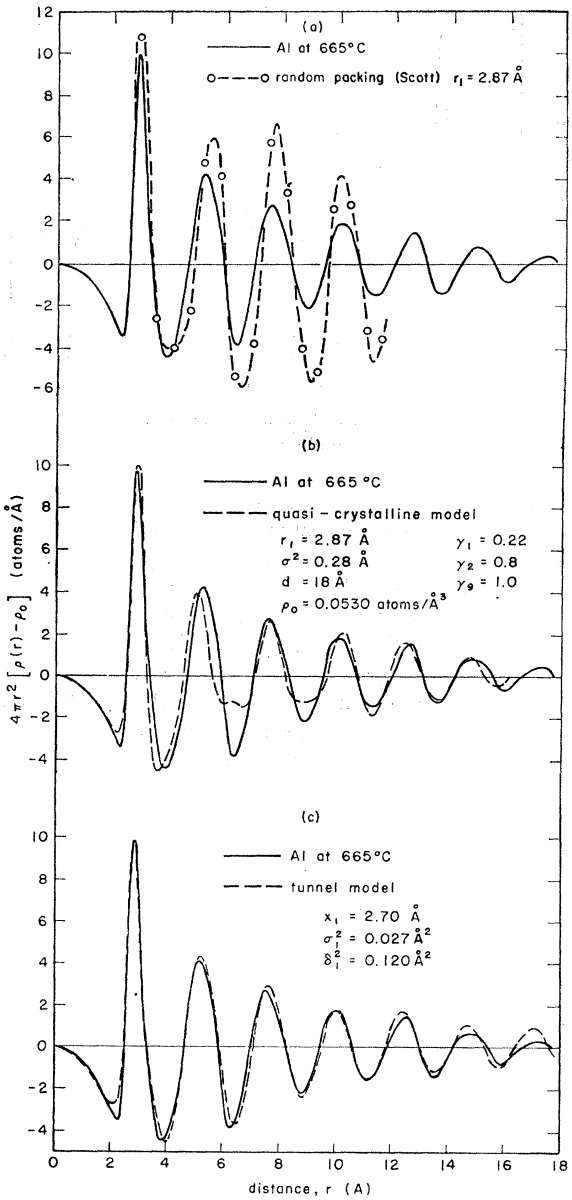

FIG. 10. The radial density function of liquid aluminum compared with the random packing, quasicrystalline, and tunnel models.

function of randomly packed spheres measured by Scott.[19] A value of 2.87 Å for the sphere diameter was chosen to make the positions of the oscillations in the two curves coincident. Although the random packing density function exhibits the general features of a liquid, it deviates greatly from the experimental function. However, Scott has indicated standard deviations for his measurements which are greater than the disagreement shown in Fig. 10(a). Thus, a more accurate determination of the density function of randomly packed spheres is required before the validity of the random packing model can be judged. In addition, determinations at smaller intervals of r are required in order to better define the shapes of the oscillations. However, even if more accurate measurements of the random packing density function reproduce the density function of liquid aluminum, it will still be necessary to introduce other factors in order to account for the density functions of more complex liquids, such as mercury.

According to the quasicrystalline model proposed by Kaplow, Strong, and Averbach,[6] the theoretical liquid radial density function may be generated by broadening and damping the corresponding function for the solid structure. The broadening and damping functions are used to account for diffusive motion in the liquid and the breakdown of long-range correlations in the atomic positions. The damping function is calculated assuming nearly spherical coherent domains with a critical diameter d. The mean-square displacements in the liquid are assumed to include both thermal and diffusive displacements, and the corresponding coupling coefficients apply to these combined displacements. The resultant density function of the quasicrystalline model is compared with the experimental function in Fig. 10(b). The values of the parameters required for this model are listed in Table I, along with the parameters which produced a comparable fit to the 750°C aluminum density function. It can be seen that the fit is good, but several discrepancies exist. The experimental dips near 6 and 9 Å are not completely reproduced, and the peaks at 5 to 10 Å are slightly shifted from the correct positions; in addition, the first peak of the model is symmetric, while the experimental first peak is asymmetric.

The final model to be considered is the tunnel model proposed by Barker.[20] It is assumed that atoms in a liquid move in nearly straight lines through tunnels formed by other atoms moving in adjacent parallel lines. The lines of atoms are arranged in a close-packed two-dimensional network, and the position of an atom

TABLE I. Parameters of quasicrystalline model for liquid aluminum. r_1=nearest-neighbor distance. σ^2=relative mean-square atomic displacement at large distances. d=critical domain diameter. γ_i=coupling factors.

Parameter	665°C	750°C
r_1	2.87 Å	2.87 Å
σ^2	0.28 Å^2	0.30 Å^2
d	18 Å	17 Å
γ_1	0.22	0.22
γ_2	0.8	0.8
γ_3	0.7	0.7
γ_4	0.8	0.8
γ_5–γ_8	0.9	0.9
γ_9–γ_∞	1.0	1.0

[19] G. D. Scott, Nature 194, 95b (1962).

[20] J. A. Barker, *Lattice Theories of the Liquid State* (Pergamon Press, Ltd., Oxford, 1963).

in any one line is independent of atom positions in adjoining lines. An atom in a given line can be vibrationally displaced with respect to atoms in the same line, and lines can be displaced with respect to one another. Barker[21] was able to calculate the thermodynamic properties and a radial density function for liquid argon, and these are in good agreement with experimental results at high liquid densities. His method of calculation, however, requires a knowledge of the pair potential, which is less well established for metals than it is for argon.

The geometrical aspects of the model are sufficiently prescribed, however, to allow trial fitting of experimental density functions if certain unknown quantities are introduced as free parameters. These parameters include: (a) the average atomic separation distances along the lines z_i; (b) the distances between lines x_i, where x_1 is assumed to be equal to z_1; (c) broadening parameters δ_i which are the r.m.s. displacements between ith neighbors in a given line; (d) broadening parameters σ_i, which are the r.m.s. displacements between ith-neighbor lines. Both broadening functions are assumed to be Gaussian.

It was convenient to use cylindrical coordinates, where the z axis is coincident with one of the lines of atoms (the origin line) and the quantities x and ϕ specify the distance and the angle, respectively, in the plane normal to the z axis. Since it is assumed that there are no z-direction correlations between atoms in different lines, and since a spherical averaging is ultimately required, the model can be replaced by one in which the origin line of atoms is surrounded by concentric cylinders of radii x_i, and coordination number n_i, with each cylinder having uniform density in the z direction. Taking a reference atom in the origin line, it is convenient to first consider the contributions to the distribution function of the atoms in the origin line and then the concentric cylinders of uniform density.

The first term is

$$4\pi r^2\rho^0(z)=\sum_{i=1}^{\infty} 2/(2\pi\delta_i^2)^{1/2}\exp[-(z-z_1)^2/2\delta_i^2], \quad (7)$$

where $\rho^0(z)$ is the density of atoms in the origin line. The z coordinate in this equation is equivalent to the radial distance r. The contribution of the cylinders requires a spherical average of the density term

$$\rho^c(z,x)=\sum_{i=1}^{\infty} K_i\exp[-(x-x_i)^2/2\delta_i^2], \quad (8)$$

where the normalizing constant K_i is

$$K_i=n_i/[2\pi z_1 x_i(2\pi\sigma_i^2)^{1/2}]. \quad (9)$$

Although the z coordinate does not appear in Eq. (8), it enters implicitly when $\rho^c(r)$ is computed, since $r=(x^2+z^2)^{1/2}$. The total density function, $4\pi r^2\times(\rho^0(r)+\rho^c(r))$, may be written as

$$4\pi r^2\rho(r)=\sum_{i=1}^{\infty} 2/(2\pi\delta_i^2)^{1/2}\exp[(r-z_i)^2/2\delta_i^2]$$

$$+\sum^{\infty} 2K_i\int_0^r \exp\{-[(r^2-z^2)^{1/2}-x_i]^2/2\sigma_i^2\}dz. \quad (10)$$

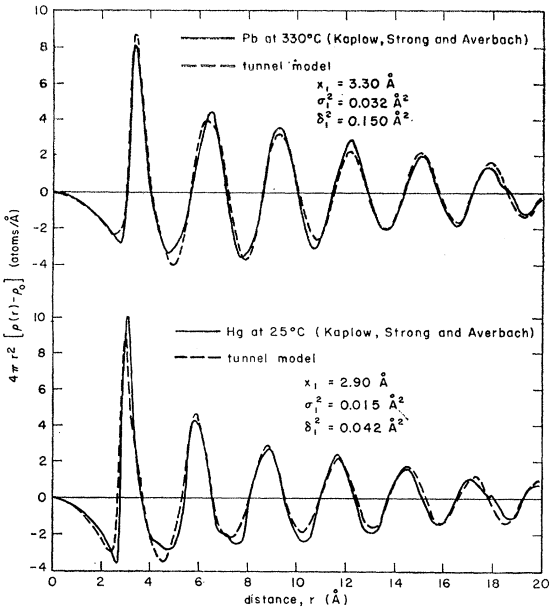

FIG. 11. Tunnel-model representation of liquid lead and mercury.

The resultant radial density function, calculated by using values of n_i, x_i, σ_i^2, and δ_i^2 to best fit the experimental results, is shown in Fig. 10(c). The structures of liquid lead and mercury, determined by Kaplow, Strong, and Averbach,[6] are also compared with the tunnel model in Fig. 11. It is evident that the agreement between the tunnel model and experimental results is excellent, even regarding the asymmetric shapes of the first peaks. The set of n_i and x_i for liquid aluminum and lead corresponds to lines of atoms located at the points of a two-dimensional lattice which has two equal basis vectors separated by an angle of 60°, as originally assumed by Barker. However, the angle between the basis vectors had to be increased to 70° in order to provide a set of n_i and x_i which would fit the distribution function of liquid mercury. Although it was obvious from the direct comparison of the experimental results that different structural bases for the model would be required to fit aluminum and mercury, it is striking that the angles derived from the fit are almost precisely the bond angles in the respective solid lattices. The broadening parameters, for both elements, for the atoms in the origin line are listed in Table II,

[21] J. A. Barker, J. Chem. Phys. **37**, 1061 (1962).

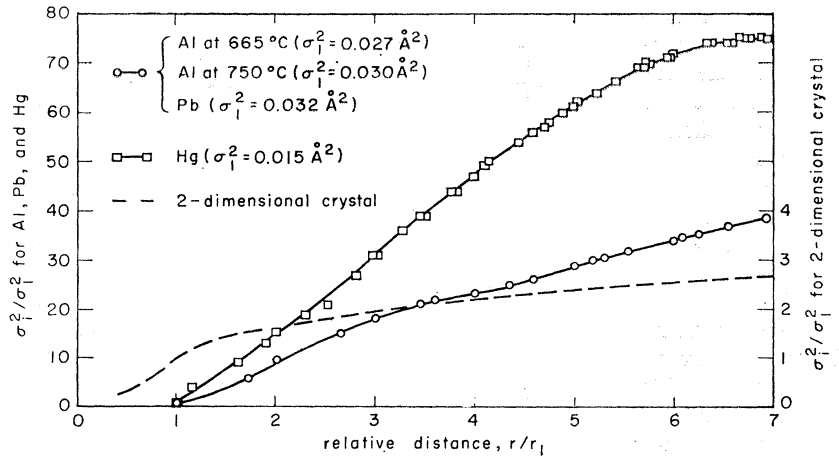

FIG. 12. Cylinder broadening parameters for the tunnel model.

and the broadening parameters for the cylinders of atoms are shown in Fig. 12.

The agreement between the tunnel model and the experimental measurements would be much more satisfying if the values of δ_i^2 and σ_i^2 could be predicted theoretically. As one possible approach, the experimental values of δ_i^2 were compared with the mean-square amplitudes of vibration in a one-dimensional crystal and σ_i^2 with the values for a two-dimensional crystal derived by Frenkel.[22] Although the one-dimensional crystal calculations agree well with δ_i^2, the two-dimensional crystal calculations, shown in Fig. 12, do not agree with σ_i^2. However, there are at least two reasons why a two-dimensional crystal analogy might not be valid. First, the tunnel model assumption that all the lines of atoms are parallel is certainly an oversimplification. Second, Frenkel's assumption that the atom displacements can be described as the sum of independent modes is probably not valid for a liquid, as indicated by the inelastic neutron scattering experiments of Rahman *et al.*[23]

Although theoretical justification has not been found for predicting the broadening parameters of the tunnel model, the concept of the model is appealing for several reasons. It has been used to make good predictions of the thermodynamic properties of liquid argon, and it can reproduce measured radial density functions very well. Because the model is based on a liquid structure which is different from solid structures, it allows for contraction upon melting for materials with very loose crystalline lattices, and it raises no controversy about the ability of liquids to be supercooled. Finally, the basic feature of the model, that of correlated diffusive motion, is identical with the mechanism of melting proposed by Kaplow, Strong, and Averbach.[13]

TABLE II. Tunnel-model broadening parameters for atom positions in the origin line. δ_1^2 (Al at 665°C) = 0.120 Å^2. δ_1^2 (Al at 750°C) = 0.123 Å^2. δ_1^2 (Pb) = 0.150 Å^2. δ_1^2 (Hg) = 0.042 Å^2.

Atom number i	δ_i^2/δ_1^2 Al and Pb	Hg
1	1.0	1.0
2	2.5	4.2
3	4.0	6.7
4	6.0	10.0
5	7.7	13.0
6	9.4	15.7
7	11.0	18.3

V. SUMMARY AND CONCLUSIONS

X-ray diffraction patterns from solid aluminum at 25, 325, and 655°C and from liquid aluminum at 665 and 750°C were analyzed to produce radial distribution functions. The analysis attempted to remove termination errors and systematic errors arising from probable errors in the scattering factors, Compton scattering, and normalization procedures.

The corrected experimental distribution functions of solid aluminum were matched with distribution functions calculated from a model in which thermal vibrations are described as a coupled Gaussian motion. Values of the lattice parameter and the Debye temperatures agreed well with other measurements of these quantities. The coupling factors exhibited a rather large scatter, indicating that the termination and high-angle error analysis of the data for the solid was probably not perfect, but when averaged over all the runs, the coupling factors agreed with theoretical predictions within the accuracy of the experiment.

The measured liquid radial density functions showed that the effect of temperature on the structure of liquid aluminum is small over the temperature range studied. There seems to be a correlation between the solid and liquid structures of metals, because liquid aluminum has the same basic structure as liquid lead but has a distinctly different structure than liquid mercury. The structure of liquid aluminum was also

[22] J. Frenkel, *Kinetic Theory of Liquids* (Dover Publications, Inc., New York, 1955), p. 123.
[23] A. Rahman, K. S. Singwi, and A. Sjolander, Phys. Rev. **126**, 997 (1962).

compared with several models. There was qualitative but not quantitative agreement with the random packing model. There was reasonably good agreement with the quasicrystalline model, except for the precise shape of the first peak and two extra oscillations in the calculated density function. A method was devised for calculating radial density functions using the assumptions of the tunnel model. The calculated density functions agreed very well with experimental measurements, but the results are based on parameters which cannot be predicted theoretically at this time. Nevertheless, the tunnel model possesses enough features to warrant further investigation.

ACKNOWLEDGMENTS

The authors would like to acknowledge the Office of Naval Research for their support of this research and the MIT Computation Center for their support of the phases of the work which involved the computer. They are specially indebted to S. L. Strong for his assistance throughout the course of the research.

PHYSICAL REVIEW VOLUME 150, NUMBER 1 7 OCTOBER 1966

Resonant Electron-Capture Measurements of Close He^{++}—He and He^{++}—H Collisions*

WILLIAM C. KEEVER AND EDGAR EVERHART
Physics Department, The University of Connecticut, Storrs, Connecticut
(Received 25 May 1966)

Differential measurements of close single collisions are made for the reaction $He^{++}+He \rightarrow He+He^{++}$ in which the probability P_0 for double electron exchange is found to be an oscillating function of incident energy. Similar measurements for the reaction $He^{++}+He \rightarrow He^{+}+He^{+}$ show that the probability P_1 for exchange of a single electron (plotted versus reciprocal velocity) oscillates at twice the frequency of the P_0 oscillations. Close encounters in the one-electron collision $He^{++}+H \rightarrow He^{+}+He^{+}$ are also studied here, and the probability P_1 of electron exchange plotted versus energy shows an oscillation of low amplitude. The experiments encompass incident He^{++} energies in the range of 2 to 200 keV and scattering angles between 1.2° and 3.0°. The data are discussed using energy-level diagrams of the $HeHe^{++}$ and HeH^{++} systems.

I. INTRODUCTION

EXPERIMENTS studying close encounters in ion-atom collisions have shown resonant electron capture phenomena to occur in a number of symmetrical ion-atom combinations.[1] The present experiment shows that there is a similar phenomenon in He^{++}–He collisions which might be termed resonant *double* electron capture. In the reaction

$$He^{++}+He \rightarrow He+He^{++}, \quad (1)$$

the fast alpha particle picks up both electrons in a single close encounter and the probability for double capture is here found to be a resonant or oscillating function of incident energy.

This phenomenon in the He^{++}–He system was predicted by Lichten[2,3] and by Basu, Mukherjee, and Sil.[4] It is shown here that the predictions[2–4] regarding spacings (versus reciprocal velocity) of the capture-probability peaks are in good qualitative agreement with the data. Lichten[2] made the further remarkable prediction that the *single* electron-capture probability in the competing reaction

$$He^{++}+He \rightarrow He^{+}+He^{+} \quad (2)$$

would oscillate with twice the frequency of the *double* electron-capture probability. This prediction by Lichten is indeed borne out by the present data.

Measurements of the unsymmetrical He^{++}–H combination are also presented. This is, after H^{+}–H, practically the only other one-electron combination which it is feasible to study.[5] This combination is accidentally resonant (with zero energy deficit) according to

$$He^{++}+H(1s) \rightarrow He^{+}(2s \text{ or } 2p)+H^{+} \quad (3)$$

if the incident particle is left in an $n=2$ state after the

* This work was sponsored by the U. S. Army Research Office, Durham, North Carolina.

[1] Experimental work: H^{+}–H: G. J. Lockwood and E. Everhart, Phys. Rev. **125**, 567 (1962); H. F. Helbig and E. Everhart, *ibid.* **140**, A715 (1965); He^{+}–He: G. J. Lockwood, H. F. Helbig, and E. Everhart, *ibid.* **132**, 2078 (1963); D. C. Lorents and W. Aberth, *ibid.* **139**, A1017 (1965). Other experiments and the related theoretical papers are discussed in the above papers.

[2] W. Lichten, Phys. Rev. **131**, 229 (1963).

[3] W. Lichten, Phys. Rev. **139**, A27 (1965).

[4] D. Basu, S. C. Mukherjee, and N. C. Sil, in *Proceedings of the Third International Conference on Physics of Electronic and Atomic Collisions, London, 1963*, edited by M. R. C. McDowell (North-Holland Publishing Company, Amsterdam, 1964), p. 769.

[5] Almost the only other one-electron combinations are Li^{+++}–H and He^{+}–H^{+}, both of which would offer great difficulties for these differential-cross-section measurements.